Small-Angle Neutron Scattering Studies of Different Mixed Micelles Composed of Dimeric and Monomeric Cationic Surfactants

Soma De,[†] Vinod K. Aswal,[‡] Prem S. Goyal,[‡] and Santanu Bhattacharya*[,†]

Department of Organic Chemistry, Indian Institute of Science, Bangalore 560 012, India, and Solid State Physics Division, Bhabha Atomic Research Centre, Bombay 400 085, India

Received: October 31, 1996; In Final Form: April 14, 1997[⊗]

Measurements of small-angle neutron scattering (SANS) cross sections from different mixed micelles composed of CTAB and Br^-, n-$C_{16}H_{33}N^+Me_2$−$(CH_2)_m$$N^+Me_2$−$n$-$C_{16}H_{33}$, Br^- (16-m-16, $2Br^-$, where m = 3, 5, and 10), in aqueous media (D_2O) are reported. The data have been analyzed using the Hayter and Penfold model for macroion solution to compute the interparticle structure factor $S(Q)$ taking into account the screened Coulomb interactions between the micelles. The aggregate composition matches with that predicted from an ideal mixing model. The SANS analysis further indicates that the extent of aggregate growth and the variations of shapes of the mixed micelles could be modulated by the amount of dimeric surfactant present in these mixtures. With the spacer chain length $m \leq 4$ in the dimeric surfactant, the propensity of micellar growth is particularly pronounced. The effect of the variation of the temperature for the mixed micellar system (23.1 mol % of 16-3-16, $2Br^-$) was also examined. The systemic microviscosities that the mixed micellar aggregates offer to a solubilized, extrinsic fluorescence probe, 1,6-diphenyl-1,3,5-hexatriene, were determined. The variation of the microviscosities of the mixed micelles as a function of percentages of the dimeric surfactants could be explained in terms of conformational variations and progressive looping of the spacer chain of dimeric surfactants in mixed micellar aggregates with increasing m values.

Introduction

Micelles are generally formed upon dispersion of *single-chain* surfactants in water, e.g. **1**, cetyltrimethylammonium bromide (CTAB). Another class of surfactant called *dimeric* or *gemini* surfactants has recently been introduced.[1] They are made of two hydrophobic chains and two polar headgroups covalently attached through a spacer, e.g. **2**. Micelles of these dimeric surfactants, especially with short spacers ($m \leq 4$), possess unusual properties, such as very low critical micellar concentrations, high viscoelasticities, and enhanced abilities for lowering the oil−water interfacial tension in comparison to their single-chain counterparts.[2] Consequently, these systems are of appreciable current interest.[3]

n-$C_{16}H_{33}N^+Me_3$, Br^-

1

$$n\text{-}C_{16}H_{33}\,N^+Me_2(CH_2)_m\,N^+Me_2n\text{-}C_{16}H_{33}$$
$$2Br^-$$

2

Recently, it was shown that the aqueous dispersions of the dimeric surfactants, 16-m-16, with m-value ≤ 4, have high propensity for micellar growth.[4] The dimeric surfactants with m-value ≤ 4 generally gave thread-like micelles while the ones with $m \geq 5$ generated either ellipsoidal or spherical microstructures. In contrast, the corresponding "monomeric" surfactant, CTAB, forms roughly spherical micellar aggregates even up to concentrations ca. 50 mM. Since the polar headgroups are *connected* by a covalent linkage within a gemini surfactant itself, the separation between the polar headgroups within a dimeric unit depends both on the nature (rigid vs flexible) and the length of the spacer.[4]

Aggregates formed from different surfactant systems have been examined earlier by neutron scattering.[5−8] Due to our interest in the design of new surfactants[9] and also in the studies of their aggregation behavior, we examined the small-angle neutron scattering (SANS) spectra of the micelles formed from dimeric surfactants, 16-m-16, $2Br^-$ surfactants **2**, where, m = 3, 4, 5, 6, 8, 10, and 12.[10] This SANS analysis clearly indicates that the extent of aggregate growth and the variations of shapes of the dimeric micelles depend primarily on the spacer chain length.

There are however, very few reports on the studies of mixed surfactants by SANS.[11] Studies reporting the nature of a micellar solution from a mixture of a single-chain and a double-chain surfactant 12-2-12, $2Br^-$ by SANS have appeared in literature only recently.[12] The studies of the mixed micelle formation from the surfactant mixtures of known composition are of value since the surfactants used in practical applications are usually mixtures of either homologous compounds or ionic surfactants contaminated by ionized ones with slightly shorter or longer chain lengths. Additionally, the surfactant mixtures bear potential for tertiary oil recovery and also play a pertinent role in other solubilization processes, e.g. micellar dialysis, etc. In view of such importance, mixtures of ionic and nonionic surfactants[13a,b] or mixtures of surfactants differing in the hydrocarbon chain lengths[13c,d] or in the headgroup structures[13e] have been examined in some detail. But, these studies have been largely confined to the determination of the critical micellar concentration (cmc),[13f,g] Krafft points,[13h] and cloud points[13i] of the mixed micelles and the counterion binding of mixed micelles.[13e] Equimolar mixtures of solutions of various *oppositely charged* surfactants have also been examined very recently.[14,15] We thought that it would be worthwhile to examine the mixed micelles from 16-m-16, $2Br^-$ and CTAB (monomeric surfactant of identical chain length). This may also

* To whom the correspondence should be addressed. Also at the Chemical Biology Unit, Jawaharlal Nehru Centre for Advanced Scientific Research, Bangalore 560 064, India.
[†] Indian Institute of Science.
[‡] Bhabha Atomic Research Centre.
[⊗] Abstract published in *Advance ACS Abstracts,* June 1, 1997.

S1089-5647(96)03402-5 CCC: $14.00

allow the long ellipsoidal micelle due to 16-*m*-16, $2Br^-$ to undergo a transition to a more sphere-like micelle in the resulting mixed micelles.

In this paper, we report the results of our SANS studies on the mixed micelles of known compositions of CTAB and various dimeric surfactants, 16-*m*-16, $2Br^-$. To elucidate the effects of the spacer chain length of the 16-*m*-16, $2Br^-$ in the aggregation properties of the resulting mixed micelles with CTAB, different dimeric surfactants with $m = 3$, 5, and 10 were employed with CTAB at similar molar ratios. The effect on SANS spectra as a function of temperature was also examined for a mixed micellar solution at a fixed molar ratio of CTAB and 16-*m*-16, $2Br^-$. The effect of *m*-values of the dimeric surfactant on the apparent microviscosities for different mixed micellar solutions have also been described.

Experimental Section

Materials. Cetyltrimethylammonium bromide (CTAB) was purchased from Aldrich Chemical Co. and was recrystallized before use. All the dimeric surfactants 16-*m*-16, $2Br^-$, $m = 3$, 5, and 10, were prepared as described.[10] All of these new surfactants gave ^1H NMR spectra and elemental analysis data consistent with their assigned structures. All the reagents and solvents were the highest grade available commercially and were used purified, dried, or freshly distilled as required. Steam distilled water was used for all physical measurements.

Methods. Fluorescence Measurements. Fluorescence technique was used to determine the critical micellar concentrations. Pyrene (Aldrich Chemical Co.), a fluorescence probe of the spectral signature of that changes with the formation of the micelle, was chosen as a probe. Steady-state fluorescence measurements were done in a Hitachi F-4500 fluorescence spectrophotometer equipped with a thermostated water-circulating bath (Julabo Model F10). All the measurements were carried out at 30 °C and used a 3 cm^3 cell. Excitation wavelength was fixed at 337 nm, and emission spectra of the region 360−410 nm were studied. Bandwidths were fixed at 5 nm for both the emission and excitation spectra. Mixed surfactant solutions of different compositions in water were doped with pyrene for the cmc determinations. Then from the plots of the concentration of the mixed micellar solution vs the ratio (I_3/I_1) of the intensities of the first (I_1) and the third (I_3) vibronic peaks in the fluorescence emission spectra due to solubilized pyrene, the cmc values were determined.[16]

Determination of Microviscosities ($\bar{\eta}$). The fluorescence anisotropies (*r*) of 1,6-diphenyl-1,3,5-hexatriene (DPH), as sensed by DPH doped in mixed micelles, were measured from the intensities obtained at 0−0°, 0−90°, 90−0°, and 90−90°angle settings of the excitation and emission polarization accessories, respectively. The temperature of the cuvette containing the sample was maintained at 30 °C or at any other temperature with the aid of a thermostated temperature-controlling water-circulating bath (Julabo Model F10). The fluorescence intensities of the emitted light polarized parallel ($I_{||}$) and perpendicular ($I_\perp$) to the exciting light were recorded and were corrected for the scattered light intensity, which was determined independently for an unlabeled reference suspension by the same procedure. The fluorescence anisotropy (*r*) for each mixed micellar sample at 30 °C was calculated according to $r = (I_{||} - GI_\perp)/(I_{||} + 2GI_\perp)$, where *G* is the grating correction factor. Microviscosities ($\bar{\eta}$) of the individual mixed micellar systems in which the fluorophore was placed were calculated from the anisotropy values.[17] The measurements were done for the same compositions at which SANS was studied.

Determination of the Compositions of the Mixed Micelles. For the calculation of the composition, Clint's theoretical treatment has been employed, which assumes an ideal mixing of the surfactant components, which in turn makes it possible to calculate monomer concentrations and micelle compositions above the cmc of the mixed micellar system under examination. On the basis of this model of Clint,[13d] the mixed cmc (c_m), unaggregated monomer concentrations (c_1^m and c_2^m), and the mole fraction of surfactant **1** (CTAB) in the mixed micelle (x_1) as a function of the total surfactant concentration are calculated from the cmc's of the pure components and the bulk mole fraction of the component 1 in the surfactant mixture by

$$1/c_m = \tau/c_{m1} + (1 - \tau)/c_{m2} \quad (1)$$

$$c_1^m = \{-(c - \Delta_{cmc}) + [(c - \Delta_{cmc})^2 + 4\tau c\Delta_{cmc}]^{1/2}\}/2(c_{m2}/c_{m1} - 1) \quad (2)$$

$$c_2^m = (1 - c_1^m/c_{m1})c_{m2} \quad (3)$$

$$x1 = (\tau c - c_1^m)/(c - c_2^m - c_1^m) \quad (4)$$

where τ is the mole fraction of the surfactant, **1** in the total mixed solute; c_{m1} and c_{m2} are the cmc's of the pure individual surfactants **1** and **2**; Δ_{cmc} is $(c_{m2} - c_{m1})$; and c is the total surfactant concentration.

Small Angle Neutron Scattering (SANS) Measurements. SANS is a well-established technique to investigate the structural aspects of materials on a length scale of 10−1000 Å.[18] As reported earlier,[5−7,13a] SANS measurements provide useful information pertaining to the shapes of various self-organizing systems in a noninvasive manner. Recently, we examined the role of spacer chain length (*m*) on the morphology of dimeric micelles using the SANS experiments.[10] To extract more information about them, we have now carried out their SANS studies with the dimeric surfactant 16-*m*-16, $2Br^-$ in the presence of the corresponding monomeric surfactant, CTAB, under mixed micellar conditions.

The SANS experiments were carried out on mixed micellar systems composed of CTAB with one of the dimeric surfactants 16-*m*-16, $2Br^-$ ($m = 3$, 5, and 10). All of the final solutions used in the neutron-scattering experiments were prepared in D_2O (at least 99.5 atom % D pure). This provides a good contrast between the micelle and the solvent in a SANS experiment. Neutron-scattering measurements were performed on the 7.0 m (source-to-detector distance) SANS instrument at the CIRUS Reactor, Trombay.[19a,20] The sample-to-detector distance was 1.8 m for all the runs. This spectrometer made use of a BeO filtered beam and had a resolution ($\Delta Q/Q$) of about 15% at $Q = 0.05$ $Å^{-1}$. The angular distribution of the scattered neutrons was recorded using an indigenously built one-dimensional position sensitive detector (PSD). The detector is filled with He^3 gas and works on the principle of charge division. It has a resolution of about 9 mm. The accessible wave vector transfer, Q ($= 4\pi \sin {}^1/_2\phi/\lambda$, where λ is the wavelength of the incident neutrons and ϕ is the scattering angle), range of this instrument is between 0.02 and 0.3 $Å^{-1}$. PSD allows a simultaneous recording of the data over the full Q range. The wavelength was $\lambda = 0.52$ nm. The SANS data from the above instrument are normalized to absolute scale by comparing the data against those from Porasil A11.[21]

The solutions were held in a 0.5 cm path-length UV grade quartz sample holder with tight-fitting Teflon stoppers, sealed with parafilm. In all the measurements, the percentages of dimeric surfactants (16-*m*-16, $2Br^-$) in the micelles of binary surfactant mixtures were varied from 0 to 33.3 mol %. The sample temperature was maintained fixed at (30 ± 0.1 °C). The

effect of the temperature on the SANS distribution was also investigated for the mixed micellar system of 30 mM 16-3-16, $2Br^-$ with 100 mM CTAB.

Data Treatment. Scattering intensities from the mixed surfactant solutions were corrected for detector background and sensitivity, empty cell scattering, and sample transmission. Solvent intensity was subtracted from that of the sample. The resulting corrected intensities were normalized to absolute cross-section units, and thus $d\Sigma/d\Omega$ vs Q was obtained. This absolute calibration has an estimated uncertainty of 10%. The experimental points are fitted using a nonlinear least-squares routine as described below. The data have not been corrected for resolution effects. Analysis of a limited set of data showed that resolution corrections do not alter the aggregation number of the micelle, especially when SANS data shows a peak. The value of charge parameter α, however, increases with resolution correction. In present studies, we were largely interested in relative aggregation numbers of the two surfactants, and therefore we did not take account of resolution effects in the analysis. The comparison between the experimental and the calculated cross sections are shown in Figures 1−4. The data for $Q > 0.16$ Å^{-1} have not been shown as the signal to background ratio was very poor.

SANS Analysis. 1. Calculation of the Scattering Intensity. The coherent differential scattering cross section, $(d\Sigma/d\Omega)$, derived by Hayter and Penfold[22] and Chen[18] can be reduced to eq 5 for an assembly of *monodisperse* system of micelles

$$d\Sigma/d\Omega = nV_m^2(\rho_m - \rho_s)^2P(Q)\,S(Q) \qquad (5)$$

where n denotes the number density of the mixed micelles, ρ_m and ρ_s are, respectively, the scattering length densities of the mixed micelle and the solvent, and V_m is the volume of the mixed micelle. $P(Q)$ is the single (orientationally averaged) particle (intraparticle) structure factor and $S(Q)$ is the interparticle structure factor. For the analysis, we assume the micelles to be mono-disperse prolate ellipsoids, ($a = c \neq b$), where the sphere is a special case of that. It may be mentioned however, that elongated micelles usually tend to be of varying sizes[23] and may not be monodisperse. But eq 5 is not valid for the polydisperse system. Although we are aware of the limitations of such assumptions, it is not possible to get information on size distributions of micelles from the present data because of the involvement of too many unknown parameters in the data analysis. Thus, in the present analysis, we have assumed the system to be monodisperse to avoid additional unknown parameters. Then eq 5 can be rewritten as

$$d\Sigma/d\Omega = [(c - c_m)V_m^2(\rho_m - \rho_s)^2P(Q)\,S(Q)]/N \qquad (6)$$

where $(c - c_m) = nN$, c_m is cmc, and c is the surfactant concentration. The aggregation number N for the mixed micelle is related to the micellar volume V_m by the relation $N = V_m/v$ where v is the volume of the individual surfactant molecule.

Now, the volume of the mixed micelle may be calculated by eq 7

$$V_m = N(x_1v_{CTAB} + (1 - x_1)v_{16-m-16}) = (N_{CTAB}v_{CTAB} + N_{16-m-16}v_{16-m-16}) \qquad (7)$$

where v_{CTAB} and $v_{16-m-16}$ are the volumes of CTAB and gemini surfactant, respectively. $N = (N_{CTAB} + N_{16-m-16})$; N_{CTAB} and $N_{16-m-16}$ are the aggregation numbers of CTAB and gemini surfactant in the mixed micelle, respectively. The values of the volume used for CTAB, 16-*3*-16, $2Br^-$, 16-*5*-16, $2Br^-$, and 16-*10*-16, $2Br^-$ are 595, 1300, 1500, and 1650 Å^3, respectively.[23] The values for 16-*5*-16, $2Br^-$, 16-*10*-16, $2Br^-$, and CTAB were available from our reported study.[10] The corresponding value for 16-*3*-16, $2Br^-$ was determined by keeping it as a parameter in the mixed micellar system composed of 10 mM 16-*3*-16, $2Br^-$ and 100 mM CTAB.

The scattering length density of mixed micelle is obtained from eq 8,

$$\rho_m = (x_1\rho_{CTAB} + (1 - x_1)\rho_{16-m-16}) \qquad (8)$$

where ρ_{CTAB} and $\rho_{16-m-16}$ are the scattering length densities due to CTAB and 16-*m*-16, $2Br^-$ surfactants, respectively.

The form factor $P(Q)$ for an ellipsoidal particle is given by the eq 9, i.e.,

$$P(Q) = \int_0^1 [F(Q,\mu)]^2 d\mu \qquad (9)$$

where μ is the cosine of the angle between the axis of resolution and Q.

The form factor $F(Q,\mu)$ is given by eq 10, i.e.,

$$F(Q,\mu) = 3(\sin w - w\cos w)/w^3 \qquad (10)$$

where $w = Q[a^2\mu^2 + b^2(1 - \mu^2)]^{1/2}$ and a and b are, respectively, the semiminor and semimajor axes of the ellipsoid of revolution. That is, $P(Q)$ depends on a and b.

2. Structure Factor for Interacting Micelles. The interparticle structure factor $S(Q)$ depends on the spatial distribution of micelles. In the following analysis, we have calculated $S(Q)$ using mean spherical approximation as developed by Hayter and Penfold.[22b] This theory is applicable if there is no angular correlation between the particles. This assumption is quite reasonable for *charged* micelles especially when the surfactant concentration is low and the ratio of the axes is not much greater than unity. Strong electrostatic repulsions prohibit close proximity of two micelles. In the following, the ellipsoidal micelle is approximated by an equivalent sphere of radius $R = (a^2b)^{1/3}$. It may be mentioned that satisfactory data analysis procedures for cylindrical particles have not been developed. Though the approximation of treating an ellipsoid as a sphere has been often used in the literature,[18] its consequences on size parameters are not fully understood. The intermicellar interaction is modeled via a screened Coulomb potential, and $S(Q)$ is calculated in mean spherical approximation. In this analysis, the only unknown parameters in $d\Sigma/d\Omega$ are the effective monomer charge, α, and the aggregation number, N.

The data in Figures 1−3 (corresponding to different mixed micelles composed of any one of the dimeric surfactants, 16-*m*-16, $2Br^-$, $m = 3$, 5, and 10 with CTAB) were first analyzed in terms of eq 6. The minor axis, a, which was obtained from 100 mM CTAB at 32 °C, was kept fixed at 22 Å. N and α were taken as the parameters of the fit. The solid lines in Figures 1−3 are the calculated curves. The major axis b ($3Nv/4\pi a^2$) was obtained from a knowledge of the above parameters. The values of N, α, and b are given in Tables 1−3. The effect of temperature on size parameters was also obtained by similar methods.

Results and Discussion

Ideal mixing, combined with the pseudophase-separation model, is useful for predicting micellar composition and the amount of unaggregated surfactant for total surfactant concentrations above the cmc. Since the amount of unaggregated surfactant and the micellar composition have contributions to the structure factor and scattering amplitude calculations, we decided to have the following assumptions about the micellar

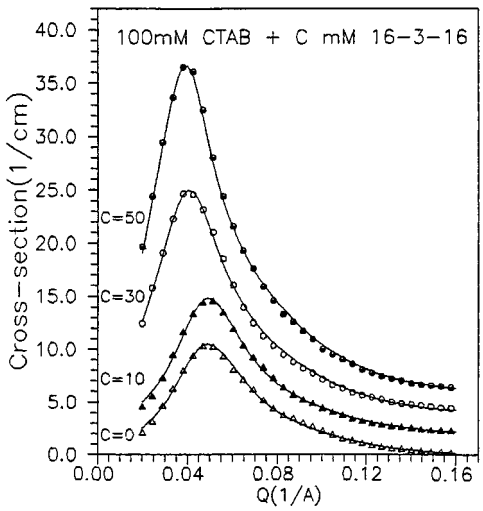

Figure 1. SANS distributions from the mixed micelles of the *C* mM 16-*3*-16, $2Br^-$ dimeric system with 100 mM CTAB at different concentrations of the dimeric surfactants, 0 mM (△), 10 mM (▲), 30 mM (○), and 50 mM (●) at 32 °C. The lines shown are theoretical fits, and the solid marks are experimentally determined data points.

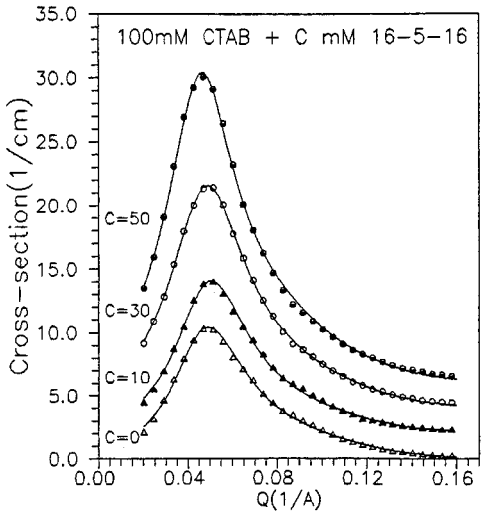

Figure 2. SANS distributions from the mixed micelles of the *C* mM 16-*5*-16, $2Br^-$ dimeric system with 100 mM CTAB at different concentrations of the dimeric surfactants, 0 mM (△), 10 mM (▲), 30 mM (○), and 50 mM (●) at 32 °C.

composition and free monomer concentration. As the experimental cmc values for the mixed micellar solutions matched well with the theoretical values, we assumed that the dimeric surfactants 16-*m*-16, $2Br^-$ mixed ideally with CTAB. Similar observation was also reported by Zana and co-workers[12] for the studies with mixed micelles of 12-*m*-12, $2Br^-$ and its corresponding monomer, dodecyltrimethylammonium bromide (DTAB). Since the polar headgroups and the counterions of 16-*m*-16, $2Br^-$ and that of CTAB are quite similar and are of same electrostatic character, the assumption of ideal mixing appears to be quite appropriate.

The SANS measurements for the mixed micellar solutions of dimeric surfactants 16-*m*-16, $2Br^-$ and CTAB (Figures 1−3) were carried out at three different compositions at 32 °C in D_2O. Measurements have covered *Q* ranges from 0.02 to 0.16 $Å^{-1}$.[25] The different compositions used were (a) 10 mM 16-*m*-16, $2Br^-$ + 100 mM CTAB, (b) 30 mM 16-*m*-16, $2Br^-$ + 100 mM CTAB, and (c) 50 mM 16-*m*-16, $2Br^-$ + 100 mM CTAB for the dimeric surfactant with a given *m*-value. For the sake of comparison, the data for a pure 100 mM CTAB solution[19] are

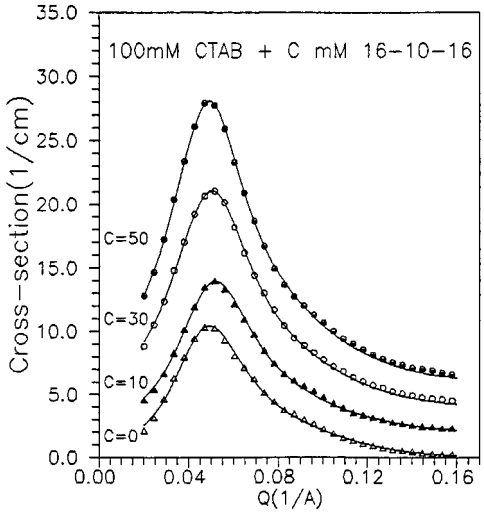

Figure 3. SANS distributions from the mixed micelles of the *C* mM 16-*10*-16, $2Br^-$ dimeric system with 100 mM CTAB at different concentrations of the dimeric surfactants, 0 mM (△), 10 mM (▲), 30 mM (○), and 50 mM (●) at 32 °C.

also shown in Figures 1−3. SANS distributions for all of them show interaction peaks characteristic of dispersions of charged particles. This peak arises because of the corresponding peak in the interparticle structure factor $S(Q)$. Usually, this peak occurs at $Q_m \sim 2\pi/d$, where *d* is the average distance between the micelles.

The mixed micellization studies were done with three different dimeric surfactants, two with spacer chains having an odd number of CH_2 groups, i.e., $m = 3, 5$, and the other with a spacer chain with even number of CH_2 groups, i.e., $m = 10$. Figure 1 shows the data for the mixed micelles of 16-*3*-16, $2Br^-$ and CTAB at 32 °C. It is seen that the calculated distributions give the peak positions in $d\Sigma/d\Omega$ with a good correspondence with the experimentally determined points. As the percentage of dimeric surfactants in the mixed micelles increases, the interparticle distance increases and the position of maximum intensity (Q_m) shifts to a lower *Q*-value with a concomitant increase in the maximum intensity. This is reflected in the equivalent aggregation number of monomers, N_m ($= N_{CTAB} + 2N_{16-m-16}$, where the dimeric surfactant has been considered to be composed of two monomers), the axial ratio (b/a) of the micelle, and the effective fractional charge (α) on micelles. N_m increases from 162 to 484, and the effective fractional charge (α) decreases, i.e., the fraction of associated counterions ($= 1 - \alpha$) increases with the increasing amount of dimeric surfactants. Since spheroids and ellipsoids differ in terms of curvature, *larger* effective charge would be expected for a *spheroidal* micelle, and *smaller* effective charge would be indicated for an *ellipsoidal* morphology. So, we find that the micellar shape changes from $b/a \sim 2.16$ to $b/a \sim 6.76$ (more prolate ellipsoidal) as the concentration of the dimeric surfactant 16-*3*-16, $2Br^-$ increases from 0 to 33 mol % in the mixed micelle (Table 1). This also suggests that a fewer number of $-CH_2-$ groups in the spacer chain protrudes into the shell when 16-*3*-16, $2Br^-$ is incorporated into the mixed micelle. This increases insignificantly when one adds 9.1 mol % of the dimeric surfactant to CTAB. However, the spacer chain looping into the shell increases appreciably beyond 9.1 mol % of the 16-*3*-16, $2Br^-$, indicating sphere → ellipsoid morphological transition. Since the shape of the mixed micelle changes as a function of the concentration of the dimeric surfactant, the interactions among the charged headgroups of the mixed micellar aggregates and water in the Stern layer region of the mixed micelle appear to

TABLE 1: Values of the Various Parameters for the Mixed Micelles of *C* mM 16-*3*-16, 2Br$^-$ and 100 mM CTAB Obtained from Fits to the Experimental Data[a]

C (mM)	*N*	N_{CTAB}	$N_{16-3-16}$	N_m[b]	effective monomer charge α	semiminor axis $a = c$ (Å)	semimajor axis *b* (Å)	*b*/*a*
0	162	162	0	162	0.102	22.0	47.6	2.16
10	171	155	16	187	0.096	22.0	55.6	2.52
30	290	223	67	357	0.060	22.0	108.6	4.94
50	363	242	121	484	0.056	22.0	148.6	6.76

[a] υ was kept fixed in the fitting procedure. [b] N_m is the equivalent aggregation number of monomers; i.e., $N_{CTAB} + 2N_{16-3-16}$, where 16-3-16 is considered to have two monomers.

TABLE 2: Values of the Various Parameters for the Mixed Micelles of *C* mM 16-*5*-16, 2Br$^-$ and 100 mM CTAB Obtained from Fits to the Experimental Data[a]

C (mM)	*N*	N_{CTAB}	$N_{16-5-16}$	N_m[b]	effective monomer charge α	semiminor axis $a = c$ (Å)	semimajor axis *b* (Å)	*b*/*a*
0	162	162	0	162	0.102	22.0	47.6	2.16
10	158	144	14	172	0.100	22.0	53.0	2.40
30	180	138	42	222	0.080	22.0	71.3	3.24
50	234	156	78	312	0.076	22.0	103.5	4.70

[a] υ was kept fixed in the fitting procedure. [b] N_m is the equivalent aggregation number of monomers; i.e., $N_{CTAB} + 2N_{16-5-16}$, where, 16-5-16 is considered to have two monomers.

TABLE 3: Values of the Various Parameters for the Mixed Micelles of *C* mM 16-*10*-16, 2Br$^-$ and 100 mM CTAB Obtained from Fits to the Experimental Data[a]

C (mM)	*N*	N_{CTAB}	$N_{16-10-16}$	N_m[b]	effective monomer charge α	semiminor axis $a = c$ (Å)	semimajor axis *b* (Å)	*b*/*a*
0	162	162	0	162	0.102	22.0	47.6	2.16
10	147	134	13	160	0.104	22.0	50.1	2.28
30	163	125	38	201	0.086	22.0	67.5	3.07
50	192	128	64	256	0.078	22.0	89.0	4.05

[a] υ was kept fixed in the fitting procedure. [b] N_m is the equivalent aggregation number of monomers; i.e., $N_{CTAB} + 2N_{16-10-16}$, where 16-*10*-16 is considered to have two monomers.

TABLE 4: Change in Average Separation between the Two Polar Headgroups within Mixed Micelles[a]

	mol %[b] of 16-*m*-16 in mixed micelles		
entry	mol %	*m*-value	avg dist., Å
1	9.1	3	7.77
2	23.1	3	7.03
3	33.3	3	6.70
4	9.1	5	7.97
5	23.1	5	7.74
6	33.3	5	7.40
7	9.1	10	8.11
8	23.1	10	7.99
9	33.3	10	7.77

[a] Calculated assuming it to be equal to $(4\pi a_{eff}2/N)^{1/2}$ where $a_{eff} = (a^2b)^{1/3}$, considering the micelles to be *ellipsoidal*. [b] A mixture of 100 mM CTAB and 10 mM 16-*m*-16, 2Br$^-$ represents 9.1 mol % of 16-*m*-16, 2Br$^-$ in mixed micelles; a mixture of 100 mM CTAB and 30 mM 16-*m*-16, 2Br$^-$ represents 23.1 mol % of 16-*m*-16, 2Br$^-$ in mixed micelles; a mixture of 100 mM CTAB and 50 mM 16-*m*-16, 2Br$^-$ represents 33.3 mol % of 16-*m*-16, 2Br$^-$ in mixed micelles.

play a crucial role in determining the shapes of the resulting mixed micellar aggregates. Similarly, the effective fractional charge (α) also changes with the concentration of 16-*3*-16, 2Br$^-$.

With the mixed micelles composed of either 16-*5*-16, 2Br$^-$/CTAB or 16-*10*-16, 2Br$^-$/CTAB also, similar trends were observed (Figures 2 and 3). Thus the micellar shape changes from *b*/*a* value of ∼2.16 to *b*/*a* ∼ 4.70 (Table 2) and from the *b*/*a* value of ∼2.16 to *b*/*a* ∼ 4.05 (Table 3) for the mixed micellar systems of CTAB/16-*5*-16, 2Br$^-$ and CTAB/16-*10*-16, 2Br$^-$, respectively. These changes are probably due to the onset of thread-like micellar morphologies with the increase in the dimeric surfactant concentration. But the extents of increase in *b*/*a* values are very different as the spacer chain length within the dimeric surfactant changes in the mixed micelles. For

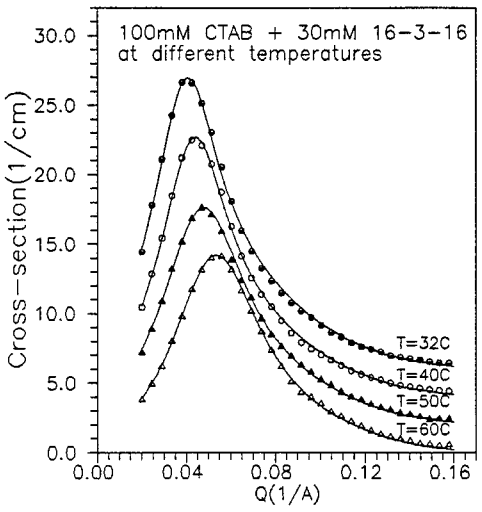

Figure 4. SANS distributions from the mixed micelles of the 30 mM 16-3-16, 2Br$^-$ dimeric system with 100 mM CTAB at various temperatures, 32 °C (●), 40 °C (○), 50 °C (▲) and 60 °C (△).

comparison, we find that the *b*/*a* value is 6.76 with the mixed micelles composed of 33 mol % of 16-*3*-16, 2Br$^-$ (50 mM) and 67 mol % CTAB (100 mM). The corresponding values at the identical composition are only 4.70 and 4.05 for the mixed micelles of CTAB/16-*5*-16, 2Br$^-$ and CTAB/16-*10*-16, 2Br$^-$, respectively. These findings clearly indicate that the propensity of the formation of prolate ellipsoidal or thread-like aggregates is more pronounced with the mixed micelles containing the dimeric surfactant with shorter spacer chain length.

Average Separation between the Two Polar Headgroups within Mixed Micelles. In aqueous solution, the two covalently connected positively charged $-NMe_2^+$ headgroups within a dimeric surfactant unit tend to maintain a critical distance

TABLE 5: Effect of Temperature on the *Q*-Values for the Mixed Micelles of 16-*3*-16, 2Br$^-$ and CTAB[a]

temp (°C)	N	N_{CTAB}	$N_{16-3-16}$	N_m[b]	effective monomer charge α	semiminor axis $a = c$ (Å)	semimajor axis b (Å)	b/a
32	290	223	67	357	0.060	22.0	108.6	4.94
40	238	183	55	293	0.065	22.0	89.3	4.06
50	183	141	42	225	0.072	22.0	68.4	3.11
60	142	109	33	175	0.091	22.0	53.0	2.41

[a] All the SANS spectra were taken using mixed micelles composed of 100 mM CTAB and 30 mM 16-*3*-16, 2Br$^-$. [b] N_m is the equivalent aggregation number of monomers; i.e., $N_{CTAB} + 2N_{16-3-16}$, where 16-*3*-16 is considered to have two monomers.

TABLE 6: Dependence of the Microviscosities of Different Mixed Micellar Systems of CTAB and 16-*m*-16, 2Br$^-$ at 32 °C

	mixed micellar system			
entry	[CTAB] (mM)	[16-*m*-16] (mM)	*m*-value	microviscosity (η)[a] (poise)
1	100	0	0	0.560
2	100	10	3	0.725
3	100	30	3	0.974
4	100	50	3	1.142
5	100	10	5	0.621
6	100	30	5	0.686
7	100	50	5	0.815
8	100	10	10	0.603
9	100	30	10	0.644
10	100	50	10	0.700

between them to minimize the Coulombic repulsion. But since such situation creates rather an unfavorable contact of the hydrophobic polymethylene spacer chain with the bulk water, a separation based on the compromise of these two opposing tendencies is resulted. We have estimated this critical distance based on the SANS data, assuming it to be equal to $(4\pi a_{eff}2/N)^{1/2}$ where $a_{eff} = (a^2b)^{1/3}$, considering the micelles to be *ellipsoidal*. Applying this, we obtained a value of $a_{eff} \sim 7.94$ Å for CTAB ($m = 0$) which is in reasonable agreement with the value reported by Zana et al.[2] In the same way, we then went ahead to calculate the critical distances between the two cationic centers for various mixed micellar systems of CTAB/16-*3*-16, 2Br$^-$. The relevant information is summarized in Table 4. Examination of the data in Table 4 suggests that the average separation between the cationic headgroups in mixed micelles decreases with an increase in the percentages of dimeric surfactant in the resulting mixture irrespective of their spacer chain length (*m*-value). However, this tendency is most pronounced for dimeric surfactants with low ($m = 3$) spacer chain length.

Effect of Temperature. While for both the conventional single-chain, and dimeric surfactant micelles considerable information is available as to how micellar size changes with the temperature, practically nothing is known about the corresponding parameter for the micelles composed of mixtures of single-chain and gemini surfactants. To secure information on this we then carried out SANS studies with mixed micelles of known composition as a function of temperature. Figure 4 shows the variation of neutron cross sections for the mixed micelles composed of 16-*3*-16, 2Br$^-$ (23.1 mol %) and CTAB as the temperature is increased. The peak in the measured distribution shifts to higher *Q*-values and broadens with the increase in temperatures. Table 5 summarizes the information based on the above experimental findings as a function of temperature. The increase in temperature promotes a greater degree of ionization and thus effects a modification of the magnitude of electrostatic repulsion. This in turn results in a decrease in the aggregation number, *N*, upon increase in temperature. In contrast, the effective fractional charge per monomer (α) increases with increasing temperature. Since a smaller effective charge indicates a more ellipsoidal morphology, an increase in temperature should favor the ellipsoid → sphere transition for the mixed micelles of CTAB/16-*3*-16, 2Br$^-$. This is consistent with the concomitant decreases in the b/a values with increases in temperature.

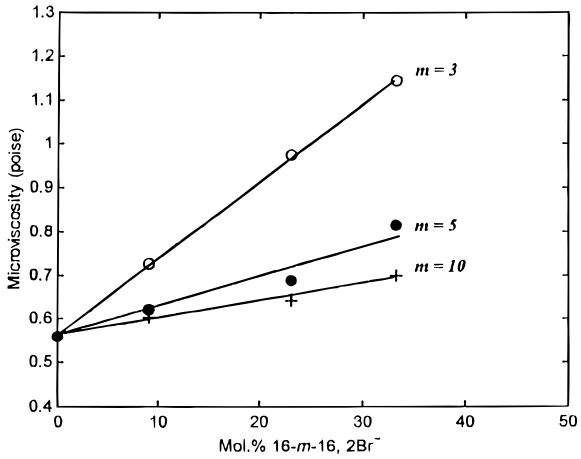

Figure 5. Variations of the microviscosities of the mixed micelles of the *C* mM 16-*m*-16, 2Br$^-$ dimeric system with 100 mM CTAB with the percentage of the dimeric surfactants at 32 °C.

Role of Spacer Chain Length of the Dimeric Surfactant on the Microviscosity ($\bar{\eta}$) of the Mixed Micelles. The microenvironmental viscosity (microviscosity, $\bar{\eta}$) of the mixed micellar aggregates is necessary to determine how it changes with the percentage and spacer chain length of dimeric surfactant. This parameter can be conveniently estimated by the determination of the fluorescence polarization of the probe 1,6-diphenyl-1,3,5-hexatriene (DPH).[16] Table 6 records the systemic microviscosity values of the 16-*m*-16, 2Br$^-$/CTAB mixed micelles at different compositions. DPH is a fluorescence probe whose emission quantum yield is enhanced upon its partitioning into a micelle or a related aggregate from water. The fluorescence polarization (*P*) or the anisotropy (*r*) values of micelle doped DPH were determined which allowed us to estimate the microviscosity ($\bar{\eta}$) of the medium in which DPH is solubilized. The microviscosity we measured in the above way agrees with that of CTAB (100 mM) reported in the literature using DPH and other probes.[26,27] Then the microviscosities for different mixed micellar systems were determined which showed a very clear trend (Figure 5). Thus as the percentage of the dimeric surfactant in mixed micelles increases, the microviscosity of the resulting aggregate also increases. However, the rate of the increase in microviscosity is more with mixed micelles containing 16-*m*-16, 2Br$^-$ of low *m*-values. This shows under these circumstances that the packing characteristics within the aggregate must be altered, which is manifested in the changeover of micellar morphology toward more ellipsoidal or rodlike structures as indicated from the previously described SANS data.

Conclusions. Investigations on the structural changes that take place in mixtures of surfactant solutions of known molecular structure and composition provide information that may be useful in predicting the nature of highly complex coaggregates. Toward this direction, to understand the nature

of coaggregates of dimeric surfactants (16-*m*-16, $2Br^-$ $m = 3$, 5, and 10) and CTAB, mixed surfactant solutions of CTAB and 16-*m*-16, $2Br^-$ were prepared at different molar proportions and the resulting mixed micelles were examined by small-angle neutron scattering. The SANS results provide useful information pertaining to the shapes and temperature dependence of representative mixed micellar systems. From the detailed measurements of SANS cross sections, we found that the dimeric surfactants 16-*m*-16, $2Br^-$ control the morphology and micellar growth in mixed micelles of dimeric surfactant−CTAB in water both as a function of the concentration of the dimeric surfactant and their *m*-values. The greater the percentage of the dimeric surfactant, the larger is the aggregation number of the resulting mixed micelles. It was also found that an increase in the spacer chain length (*m*-value) generally suppressed the tendencies of the mixed micelles toward micellar growth. Consistent with the above findings, the fluorescence studies indicate strong dependence of microviscosities on the percentage of the dimeric surfactant and its spacer chain length (*m*-value). Taken together these studies clearly demonstrate that while the micelles of 16-*m*-16, $2Br^-$ surfactants with a *short* spacer chain length ($m < 5$) tend to form nonspherical aggregates, the inclusion of CTAB in the mixed micelles with 16-*m*-16, $2Br^-$ alters the overall shape of the resulting aggregates into predominantly spherical microstructures.

Acknowledgment. We thank the Department of Atomic Energy for financial support of this work (Grant BRNS/37/11/94-R&D-II/789). We also thank Dr. B. A. Dasannacharya for his interest in this work.

References and Notes

(1) Menger, F. M.; Littau, C. A. *J. Am. Chem. Soc.* **1991**, *113*, 1451. (b) Zana, R.; Benrraou, M.; Rueff, R. *Langmuir* **1991**, *7*, 1072.

(2) Zana, R.; Talmon, Y. *Nature* **1993**, *362*, 228.

(3) Rosen, M. J. *Chemtech* **1993**, *23*, 30.

(4) Karaborni, S.; Esselink, K.; Hilbers, P. A. J.; Smit, B.; Karthauser, J.; van Os N. M.; Zana, R. *Science* **1994**, *266*, 254.

(5) (a) Berr, S. S.; Jones, R. R. M.; Johnson, J. S. *J. Phys. Chem.* **1992**, *96*, 5611. (b) Berr, S. S.; Jones, R. R. M. *Langmuir* **1988**, *4*, 1247.

(6) (a) Pilsl, H.; Hoffmann, H.; Hoffmann, S.; Kalus, J.; Kencono, A. W.; Lindner, P.; Ulbricht, W. *J. Phys. Chem.* **1993**, *97*, 2745. (b) Chevalier, Y.; Zemb, T. *Rep. Prog. Phys.* **1990**, *53*, 279. (c) Kaler, E. W.; Billman, J. F.; Fulton, J. L.; Smith, R. D. *J. Phys. Chem.* **1991**, *95*, 458. (d) Prasad, D.; Singh, H. N.; Goyal, P. S.; Rao, K. S. *J. Colloid Interface Sci.* **1993**, *155*, 415. (e) Goyal, P. S.; Menon, S. V. G.; Dasannacharya, B. A.; Thiyagarajan, P. *Phys. Rev.* **1995**, *51E*, 2308.

(7) Goyal, P. S.; Dasannacharya, B. A.; Kelkar, V. K.; Manohar, C.; Rao, K. S.; Valaulikar, B. S. *Physica B* **1991**, *174*, 196.

(8) Hirata, H.; Hattori, N.; Ishida, M.; Okabayashi, H.; Frusaka, M.; Zana, R. *J. Phys. Chem.* **1995**, *99*, 17778.

(9) (a) Bhattacharya, S.; Haldar, S. *Langmuir* **1995**, *11*, 4748. (b) Bhattacharya, S.; Snehalatha, K. *Langmuir* **1995**, *11*, 4653. (c) Bhattacharya, S.; Haldar, S. *Biochim. Biophys. Acta (Biomembranes)*, **1996**, *1283*, 21. (d) Bhattacharya, S.; Subramanian, M.; Hiremath, U. *Chem. Phys. Lipids*, **1995**, *78*, 177. (e) Bhattacharya, S.; Subramanian, M. *J. Chem. Soc., Perkin Trans. 2* **1996**, 2027. (f) Bhattacharya, S.; Snehalatha, K. *J. Chem. Soc., Perkin Trans. 2* **1996**, 2021. (g) Subramanian, M.; Mandal, S. K.; Bhattacharya, S. *Langmuir* **1997**, *13*, 153. (h) Bhattacharya, S.; Snehalatha, K. *Langmuir* **1997**, *13*, 378. (i) Bhattacharya, S.; Snehalatha, K. *J. Org. Chem.* **1997**, *62*, 2198.

(10) De, S.; Aswal, V. K.; Goyal, P. S.; Bhattacharya, S. *J. Phys. Chem.* **1996**, *100*, 11664.

(11) (a) Borbely, S.; Cser, L.; Vass, S.; Ostanevich, Yu. M. *J. Appl. Crystallogr.* **1991**, *24*, 747. (b) Lusvardi, K. M.; Full, A. P.; Kaler, E. W. *Langmuir* **1995**, *11*, 487. (c) Caponetti, E.; Chillura Martino, D.; Floriano, M. A.; Triolo, R. *Langmuir* **1993**, *9*, 1193.

(12) Schosselor, F.; Anthony, O.; Beinert, G.; Zana, R. *Langmuir* **1995**, *11*, 3347.

(13) (a) Rubingh, D. N. In *Solution Chemistry of Surfactants*; Mittal, K. L., Ed.; Plenum: New York, 1979; p 337. (b) Bucci, S.; Fagotti, C.; De Giorgio, V.; Piazza, R. *Langmuir* **1991**, *7*, 824. (c) Malliaris, A.; Binana-Limbele, W.; Zana, R. *J. Colloid Interface Sci.* **1986**, *110*, 114. (d) Velazquez, M. M.; Costa, S. M. B. *J. Chem. Soc., Faraday Trans.* **1990**, *86*, 4043. (e) Rathman, J. F.; Scamehorn, J. F. *J. Phys. Chem.* **1984**, *88*, 5807. (f) Clint, J. *J. Chem. Soc.* **1975**, *71*, 1327. (g) Asakawa, T.; Mouri, M.; Miyagishi, S.; Nishida, M. *Langmuir* **1989**, *5*, 343. (h) Moroi, Y.; Oyama, T.; Matuura, R. *J. Colloid Interface Sci.* **1977**, *60*, 103. (i) Valaulikar, B. S.; Manohar, C. *J. Colloid Interface Sci.* **1985**, *108*, 403.

(14) (a) Kaler, E. W.; Herrington, K. L.; Murthy, A. K.; Zasadzinski, J. A. N. *J. Phys. Chem.* **1992**, *96*, 6698. (b) Herrington, K. L.; Kaler, E. W.; Miller, D. D.; Zasadzinski, J. A.; Chiruvolu, S. *J. Phys. Chem.* **1993**, *97*, 13792. (c) Marques, E.; Khan, A.; da Graca Miguel, M.; Lindman, B. *J. Phys. Chem.* **1993**, *97*, 4729.

(15) (a) Bhattacharya, S.; De, S. *J. Chem. Soc., Chem. Commun.* **1995**, 651. (b) Bhattacharya, S.; De, S. *J. Chem. Soc., Chem. Commun.* **1996**, 1283.

(16) Kalyanasundaram, K. *Photochemistry in Microheterogeneous Systems*, Academic Press: New York, 1987, p 177.

(17) Shinitzky, M.; Barenholz, Y. *Biochim. Biophys. Acta* **1978**, *515*, 367.

(18) (a) Chen, S. H. *Annu. Rev. Phys. Chem.* **1986**, *37*, 351. (b) Chen, S. H.; Lin, T. L. *Methods of Experimental Physics*; Academic Press: New York, 1987; Vol. 23B, p 489.

(19) (a) At this concentration, CTAB was shown to form elongated, nonspherical micelles; see for example: Goyal, P. S.; Chakravarthy, R.; Dasannacharya, B. A.; Desa, J. A. E.; Kelkar, V. K.; Manohar, C.; Narasimahan, S. L.; Rao, K. R.; Valaulikar, B. S. *Physica B* **1989**, *156*, 471. (b) Danino, D.; Talmon, Y.; Zana, R. *Langmuir* **1995**, *11*, 1448.

(20) Goyal, P. S.; Aswal, V. K.; Joshi, J. V. BARC Report, I/018; 1995 (a report of Bhabha Atomic Research Centre, Bombay, India, 1995).

(21) (a) Wignal, G. D.; Bater, F. S. *J. Appl. Crystallogr.* **1987**, *20*, 40. (b) Dr. G. D. Wignal of the Oak Ridge National Laboratory, Oak Ridge, TN, has kindly supplied us this standard sample.

(22) (a) Hayter, J. B.; Penfold, J. *Colloid Polym. Sci.* **1983**, *261*, 1022. (b) Hayter, J. B.; Penfold, J. *Mol. Phys.* **1981**, *42*, 109. (c) Hansen, J.-P; Hayter, J. B. *Mol. Phys.* **1982**, *46*, 109. (d) Hayter, J. B.; Penfold, J. *J. Chem. Soc., Faraday Trans. 1* **1981**, *77*, 1851.

(23) The values of 595 $Å^3$ and 1300 $Å^3$ are consistent with those obtained from the Tanford formula. However, the values of the volumes of 1500 $Å^3$ and 1650 $Å^3$ are somewhat larger. Perhaps, $v = 1355$ and 1490 $Å^3$ are more acceptable values of the volumes for $m = 5$ and 10, respectively. It may be mentioned that the results of present analysis are not particularly sensitive to the value of monomer volume v. For example, the aggregation number, N and the major axis, b should be within ~4% if we use $v = 1355$ and 1490 $Å^3$ instead of 1500 and 1650 $Å^3$, respectively.

(24) Israelachvili, J. N.; Marcelja, S.; Horn, R. G. *Q. Rev. Biophys.* **1980**, *13*, 121.

(25) One expects the polydispersity in the major axis and not in the minor axis of the micelle. This information is thus contained in the low Q data and not in the high Q data. Since the signal-to-background ratio was very poor for $Q > 0.16$ $Å^{-1}$, we have not shown the data beyond $Q = 0.16$ $Å^{-1}$.

(26) Blatt, F.; Ghiggino, K. P.; Sawyer, W. H. *J. Phys. Chem.* **1982**, *86*, 4461.

(27) Chattopadhyay, A.; London, E. *Anal. Biochem.* **1984**, *98*, 469.